Experiences of studying airborne wear particles from road and rail transport

Saeed Abbasi, Ulf Sellgren, Ulf Olofsson

Department of Machine Design, KTH Royal Institute of Technology, SE 10044, Stockholm, Sweden

Corresponding author's email address: sabbasi@md.kth.se

ABSTRACT

Airborne particles and their adverse effects on air quality have been recognized by humans since ancient times. Current exhaust emission legislations increase the relative contribution of wear particles on the PM levels. Consequently, wear-based particle emissions from rail and road transport have raised concerns as ground transportation is developing quickly. Although scientific research on airborne wear-based particles started in 1909, there is almost no legislation that control the generation of wear-based particles. In addition, there is no accepted and approved standard measurement technique for monitoring and recording particle characteristics. The main objective of this study is to review recent experimental work in this field and to discuss their set-ups, the sampling methods, the results, and their limitations, and to propose measures for reducing these limitations.

Keywords:
Airborne particles, measurement, non-tailpipe, non-exhaust, wear

Nomenclature

ASR: Automatic skid reduction
APS: Aerodynamic particle sizer
CPC: Condensation particle counter
DMA: Differential mobility analyzer
EAA: Electric aerosol analyzer
EC: Elemental carbon
EDX: Energy-dispersive X-ray spectroscopy

EMU: Electric multiple unit
FESEM: Field emission scanning electron microscopy
ICP-MS: Inductively coupled mass spectroscopy
LM: Low metallic
NAO: Non-asbestos organic
NRMM: Non-road mobile machinery
OC: Organic carbon
PIXE: Proton-induced X-ray emission
PMC: Particle mass concentration
PMD: Particle mass distribution
PNC: Particle number concentration
PND: Particle number size distribution
PVD: Particle volume size distribution
SFU: Stacked filter unit
SDI: Small deposit impactor
SMPS: Scanning mobility particle sizer
TEOM: Tapered element oscillating microbalance
TOR: Thermal optical reflectance
VSD: Volume size distribution
VTI: The Swedish National Road and Transport Research Institute

1. Introduction

Solid particles or liquid droplets suspended in a gas or another fluid is referred to as particulate matter (PM). The common adverse effects of PM are health problems for humans and animals, negative visibility effects, and effects on local and global climate. These adverse effects have for long been known and recognized, although they were not prioritized in the past history. For example, King Tukulti-Ninurta II (890–884 BC) of Assyria complained of a strange smell in the air during a visit to Hit, a town west of Babylon and the centre of asphalt mining (Hopke, 2009). Currently, the PM level is a crucial factor in both the EU and US outdoor air quality standards. Table 1 shows a summary of these regulations. These standards were defined to warn decision makers about the amount of man-made PM and encourage them to devise mitigation strategies for controlling and reducing hazardous PM emissions.

Table 1. Comparison of PM levels in US and EU outdoor air quality regulations

		PM$_{2.5}$ (µg m^{-3})	PM$_{10}$ (µg m^{-3})
US EPA NAAQS	Daily (24 h)	35	150
	Annual	12	–
EU directive 2008/50/EC	Daily (24 h)	–	50 [b]
	Annual	25	40

[a]The rolling three-month average.
[b]The limit 50 µg m^{-3} must not be exceeded more than 35 times a calendar year.

Generally, man-made particles in ground transport have two main sources: exhaust, mainly from diesel engines, and wear, mainly from contact between two bodies in sliding and/or rolling contact. Wear-based particles are also known as non-exhaust particles or non-tailpipe emissions.

Most research and strategies have, so far, focused on exhaust-based particles. Euro VI emission, Tier 4 and 97/68/EC NRMM directive for rail vehicles and Euro V and VI , Tier 2 and JC 08 in road vehicles are among recent legislations setting limits on the PM contained in engine exhausts. However, the amount of research and legislation setting limits on wear-based PM emissions is very limited. Note that, though the investigation of wear-based particles began in 1909, effective action has yet to be taken, mainly because of a lack of relevant knowledge (Abbasi *et al.*, 2012a, b).

The main sources of wear-based particles in road transport are brake wear, tyre wear, and road surface abrasion (Thorpe and Harrison, 2008). The main sources of these particles in rail transport are the contacts between wheels and rails, within switches, from braking material, natural erosion, and the forces exerted by the piston effect on masonry infrastructure (Abbasi,

2011). Besides a lack of legislation, no standard measurement technique for measuring and monitoring wear particles from road and rail transport has been accepted and approved. The main objective of the present study is to review the set-ups, results, and limitations of recent and state-of-the-art measurement techniques.

2. Method

A computerized word search method was utilized in this review, mainly because it is a fast and efficient method. We limited the search to articles published in English in the last 10 years. The key words used in the initial search were "airborne", "brake", "debris", "dust", "emission", "non-exhaust", "non-tailpipe", "particle", "railway", "road", "traffic", "test", tunnel", and "wear". Since, exhaust-based particles were not the focus of our study, we selected the articles that were examining wear-based particles. Consequently, research with on-board measurements in cars and trains, laboratory studies using pin-on-disc machines, and tests with dynamometers were scrutinized. Stationary studies in tunnels, on subway stations, and at roads were excluded as they have recently been discussed and reported elsewhere (Abbasi *et al*, 2012a, Thorpe and Harrison, 2008).
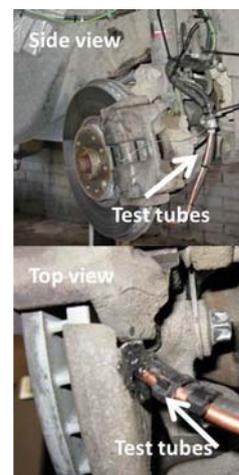
3. Results

3.1. Field studies

Wahlström et al. (2010b) reported a series of field tests using an instrumented car and focusing on dust from disc brakes. In this study, a passenger car was instrumented with different particle detection instruments. The instruments were able to record particles emitted by sampling them through collector test tubes installed at sampling points (Fig. 1).

Two sampling points were located at the front of the passenger car to measure background PM levels. Another sampling point was located directly behind the brake pad on the piston side (Fig. 1). This was an anisokinetic sampling as the car speed was not constant.

Two Grimm devices and a DustTrak aerosol monitor were used to measure particle characteristics in the background air and in the air near the brake pad. The Grimm 1.109 aerosol spectrometer (Grimm Aerosol Technik, Ainring, Germany) measures the PNC and PND of airborne particles 0.25–32 µm in diameter in 31 size intervals and concentrations of $1–2 \times 10^6$ particles L^{-1}. The DustTrak 8520 laser photometer (TSI, Shoreview, MN, USA) measures the concentration of particles roughly corresponding to the respirable size fraction, i.e., mainly in the 0.1–10 µm diameter range. A piezoelectric sensor and a K-type thermocouple sensor was used to measure brake cylinder pressure and brake pad temperature, respectively.

**Fig. 1** Side view and top view of collector tubes in an instrumented car (Wahlström *et al.*, 2010b)

This instrumented car was run in highway, country road, and heavy traffic during rainy days in Stockholm. The rainy days were chosen deliberately to compensate for re-suspension effects. According to this work, the particle size peaked at approximately 0.3–0.5 µm and the effect from an increased brake pressure was an increased total number of recorded particles.

A series of similar tests has also been conducted by instrumenting an EMU train (Abbasi *et al.*, 2012c).

Also here, two sampling points were deployed, one located 145 mm from the main brake pad and the other in the middle of the axle (Fig. 2).
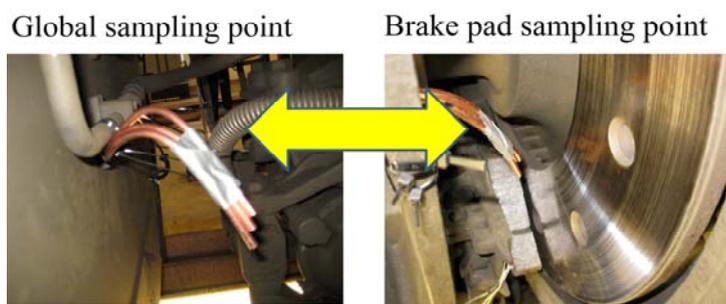
Fig. 2. A view of test tubes in the instrumented train (Abbasi *et al*, 2012c)

As the first sampling point was greatly affected by particles from the brake pad (during braking) and the wheel–rail contact (during normal operation), and the other sampling point was affected by particles from all possible sources, these points were called the brake pad sampling point and the global sampling point, respectively.

Two sets of particle sampling instruments were used, as in previously mentioned work (Wahlström *et al.*, 2010b) . Two P-Trak 8525 ultrafine particle counters were installed alongside two Grimm 1.109 aerosol spectrometers and two DustTrak 8520 laser photometers. The 47 mm, in diameter, Millipore (Billerica, MA, USA) filters were used to study element composition and particle morphology in this test. Those filters were mounted on the Grimm devices and were analyzed using ICP-MS, FESEM, and EDX.

A 340 km rail route was used for four runs over three days. Part of this route was a low-traffic track that permitted a deliberate deactivation of the electromagnetic brakes. The maximum operational speed was 90 km h^{-1} in that area. However, elsewhere on this route the train adhered

to the maximum operational speeds and here both the mechanical and electromagnetic brakes were used.

The authors identified three peaks in the fine region of the PND, i.e., for particles of 280, 350, and 600 nm in diameter. The dominant peak switched from 350 to 280 nm when the train speed increased above 70 km h^{-1}. Coarse particles were approximately 3–7 μm in diameter based on both FESEM and VSD measurements. According to ICP-MS results, excluding C, F, H, N, O, and F, the PM emitted by rail traffic comprises mainly Al, Ca, Cu, Fe, Si, and Zn. The main sources of Ca, Si, Na, and Al were suggested to be the ballast, concrete sleepers, and masonry infrastructure, because of the higher amounts of these elements captured in the global sampling point filters in all test runs. They also concluded that relative humidity has an effect on the amount of copper-based PM.

3.2. *Laboratory studies*

3.2.1. *Dynamometer studies*

A comprehensive brake dust study using a brake dynamometer was conducted by Garg *et al*. (2000), who investigated brake dust originating from seven common US-market brake pads, which were mainly semi-metallic in composition. These authors investigated the mass loss in brake pads and the amount of mass of airborne particles per stop using a brake dynamometer, i.e., a model D friction test machine (Link Engineering, Plymouth, MI, USA), following the BSL-035 brake wear procedure, which is similar to the JASO-C427-75 procedure. This procedure suggests

repeatedly braking to achieve brake disc temperatures of 100, 200, 300, and 400°C; all braking events were stop braking from an initial speed of 50 km h^{-1}. The brake assembly was located in a 14 × 18 × 36 inch chamber. A HEPA high-efficiency filter was mounted in the inlet, and the airflow was discharged through a 0.55 m diameter duct. The sampling probes were inserted into a horizontal section of this duct, 6.7 m from the brake assembly. The airflow was supplied by a computer-controlled blower and was set to 80.4, 30, 13.5, and 11.9 m^3 min^{-1} for the 100, 200, 300, and 400°C tests, respectively.

The particle measurement instruments used in this study was a classical electrical low-pressure impactor (ELPI) (Dekati, Tampere, Finland) to investigate PNC, with a 13-stage impactor for particles in the 0.03–10-µm size range, a micro orifice uniform deposit impactor (MOUDI) for investigating PMD, with a five-stage impactor for particles in the 0.1–18-µm size range, and an EAA to measure the PNC of particles larger than 0.01 µm in size.
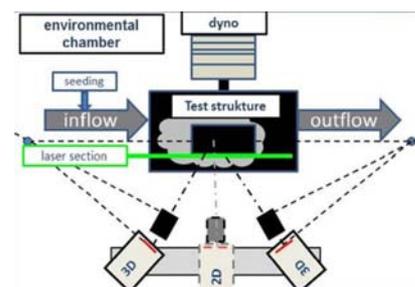
The authors used three types of filters to collect particles. A 47 mm diameter, 2 µm pore size Gelman Teflon filter was used to investigate the chemical composition using the PIXE method, which enables detection of up to 72 elements with atomic numbers greater than 10. A Pallflex 47 mm diameter Tissuquartz 2500 QAT-UP filter (Pall GmbH, Dreieich, Germany) was used to determine OC and EC with the TOR method. Mixed cellulose ester filters (MCE) with a 0.8-µm pore size were used for fibre analysis according to the NIOSH 7400 fibre counting method.

The main reported results from their work are: the brake wear rate, corresponding to the vehicle emission rate, was 3.17–8.76 mg km^{-1}. An average of 35% of the brake pad mass loss was

estimated to constitute airborne PM. The proportions of airborne particles in the PM_{10} and $PM_{2.5}$ fractions were 86% and 63%. Over 96% of total carbon was OC, accounting for 18% of the airborne PM. The fibre emissions from the brake pad material were too low to constitute an air quality issue. The PND varied significantly between brake pads and test temperatures. In addition, an increase in temperature resulted in an increase in PNC, particularly for particles smaller or equal to 30 nm as this increase was clearer in the EAA than in the ELPI. The authors also reported that differences in the wear processes and a 6.7 fold reduction in air flow explained why the proportion of airborne particles was significantly lower in the 400°C than in the 100°C test for all brake pad materials.

Brake dynamometers can also be used to study the fluid dynamics behaviour of particle clouds. In a recent study, Augsburg et al. (2011) used an NVH 3900 dynamometer (Link Engineering) along with a particle image velocimetry (PIV) system. Fig. 3 shows a schematic of their test set-up.

Fig. 3. A schematic view of the testing set-up, showing the position of the 2D + 3D PIV, the wheel house, dynamometer, and airflow direction (Augsburg et al. 2011).

The purpose of this test was to reproduce the braking conditions when braking from 150 km h^{-1} to 80 km h^{-1} at a deceleration of 0.4 g, using NAO brake pad material against a carbon ceramic disc. The authors mounted a wheel house for the dynamometer and they used wheels with different tire texture and wheel spokes. They also collected particles and analyzed them using SEM.

According to this work, the dominant particle size, as measured using SEM, was 250 nm. The authors also reported that the shape of the wheel house, the tire texture, and the number of spokes affected the air dynamic behaviour during braking in such a way that it could change the particle characteristics.

3.2.2. Pin-on-disc machine studies

The first example of using pin-on-disc machines to investigate submicron particles from braking material originates from the Howard University, USA. Mosleh *et al*. (2004) used a pin-on-disc machine with a horizontal rotating disc and an LA-700 laser scattering analyzer (HORIBA Scientific, Edison, NJ, USA) to investigate wear particles generated from a grey cast iron disk and brake pad material from a commercial truck. Two sliding velocities were used in the tests: 0.275 m s^{-1} (low speed) and 5 m s^{-1} (high speed). The tested contact pressures were 0.125, 0.375, and 0.625 MPa at low speed, and 1.0, 0.75, and 1.25 MPa at the high speed.

The authors reported peaks at 350 nm for submicron particles and at approximately 2, 7, and 15 µm for coarse particles. According to this work, 10% of the material worn off the pin and the disc became airborne particles. However, this investigation was not conducted in a testing chamber and no air was supplied to represent realistic conditions in which brake wear debris meet air when detaching from the bulk material.

Wear particles emitted from sliding contact conditions were widely studied at KTH Royal Institute of Technology, Sweden where researchers used a pin-on-disc machine with a horizontal rotating disc in a sealed chamber to simulate contact conditions between machine elements (Fig. 4).
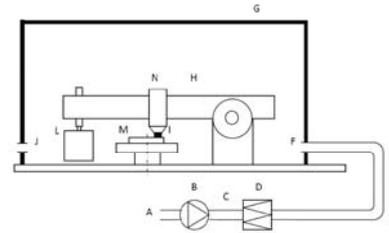
Fig. 4. Schematic of the test set-up. A: Room air; B: Fan; C: Flow rate measurement; D: Filter; E: Flexible tube; F: Clean air inlet, measurement point; G: Sealed box; H: Pin-on-disc machine; I: Pin sample; J: Air outlet, measurement points; L: Dead weight; M: Rotating disc sample, N: Air inside chamber (Olofsson *et al*. 2009).

The machine can run under stationary conditions with a constant applied normal force up to 100 N and at constant rotational speeds up to 3000 rpm. The fan (B) takes the air from the room (A) and passes it into the chamber (G) via the flow measurement system (C), filter (D), and air inlet opening (F) that is designed to monitor the cleanliness of the inlet air. Flexible tubes (E) connect the fan, measurement system, filter, and the chamber to each other. The air in the sealed chamber (N) is well mixed due to the complex shape of the pin-on-disc machine (H) and the high air-exchange rate. The mixing has been verified by analyzing the registered particle concentrations from the chamber. The air in the sealed chamber transports the particles generated in the pin-disc contact to the air outlet (J), where we find the sampling points for the particle measurement devices.

Different contact conditions, airflow rates, and particle instruments can be used in this set-up, according to the main research question that is addressed.

Sundh *et al*. (2009) used the same set-up to reproduce the slip part of a wheel–rail contact with the aim to study the relationship between wear rate and the generated airborne particles. The 50 mm diameter discs and the 17-mm-high round-head pins ($R = 5$ mm) were made from R7 railway

wheel material and UIC 60, 900 A rail material, respectively. Test series were conducted at different initial contact conditions by applying a normal load at three levels (3, 5, and 10 N), and two sliding speeds (0.1 and 0.4 m s^{-1}). To study transient effects, the normal load was increased up to 20 N during the tests. They used a P-Trak 8525 ultrafine particle counter, an SMPS (TSI, Shoreview, MN, USA), and a Grimm 1.109 aerosol spectrometer in this work. The SMPS combined model 3071 DMA and model 3010 CPC.

The authors reported that ultrafine particles, mainly with a peak at 40–80 nm in size, were generated in the wheel–rail contact, indicating thermal or chemical reactions at the asperity contact level. They also concluded that changes in sliding speed or pressure can lead to transitions between wear modes that directly affect particle generation.

Wahlström *et al*. (2010a) used a similar set-up to study wear particles from pad and cast iron rotor material from a passenger car disc brake. The 43 mm diameter discs and the 17-mm high flat-head pins (R = 10 mm) were made from a cast iron brake disc and LM and NAO brake pad materials, respectively. The sliding speed was 0.7 m s–1 and the contact pressure was 1.2 MPa. A P-Trak 8525 ultrafine particle counter, a DustTrak 8520 laser photometer, an SMPS (DMA 3071 + CPC 3010), and a Grimm 1.109 aerosol spectrometer were used in this work.

According to their results, the NAO brake pads were more aggressive and generated a higher amount of particles. They reported peaks in the PND for particles of diameters at 100, 280, 350, and 550 nm.

Olofsson (2011) used the same set-up to investigate airborne particles emitted from a railway brake block material. The 90 mm diameter discs and the 18-mm-high flat-head pins ($R = 10$ mm) were made from R7 railway wheel and organic brake blocks. In the test, the sliding speed was 0.4 m s^{-1} and the contact pressure was 0.8 MPa. He used a P-Trak 8525 ultrafine particle counter, an SMPS (DMA 3071 + CPC 3010), and a Grimm 1.109 aerosol spectrometer in this work. He also used a manual pump connected to a Nuclepore polycarbonate filter (Whatman, Maidston, UK), pore size 0.4 µm, to collect particles during the tests and studied their morphology and element composition using SEM and EDX.

The results indicated that the cast iron brake block emitted more wear particles than the organic brake block. Olofsson also reported peaks at approximately 80, 280, 350, and 550 nm in diameter in the fine region of the PND and at approximately 2 and 5 µm for particles from the cast iron brake block, whereas the peaks were found at approximately 5 and 15 µm in the coarse region of the PVD for organic brake block particles.

Further studies of airborne particles emitted from railway brake materials were conducted by Abbasi *et al.* (2011, 2012b) using the same set-up. The test used 110 mm diameter discs and 18 mm high flat-head pins ($R = 10$ mm); the discs were made from R7 railway wheel and cast iron disc material, whereas the pins were made of cast iron/organic brake block and organic/sintered brake pad materials. In the tests, sliding speeds of 8.9 m s^{-1} and 12.4 m s^{-1} – considerably higher than those used in previous tests – and contact pressures of 0.27 and 0.87 MPa where used. A P-Trak 8525 ultrafine particle counter, a DustTrak 8520 laser photometer, an SMPS (DMA 3071 + CPC 3010), and a Grimm 1.109 aerosol spectrometer were used in this work. A manual pump

connected to a Nuclepore polycarbonate filter, pore size 0.4 μm, was used to collect particles during the tests, and the morphology and element composition of the particles were analysed using SEM and EDX.

Their main documented results were as follows: Increased sliding velocities or contact pressures coincide with increased particle concentrations. The rate of ultrafine particle emissions from cast iron brake block material was significantly higher than from organic brake block material. The rate of fine and ultrafine particle emissions from sintered brake material was significantly lower than from organic brake pad material. A new index, the airborne wear particle emission rate (AWPER), was used to compare the mass of particles generated from braking material. Cast iron brake block material had a lower AWPER than organic brake block material, and sintered brake pad material had a lower AWPER than organic brake pad material. Abbasi *et al.* (2011, 2012b) suggested that the high flash temperature of the asperities and the high-surface-to-volume ratio of the spherical shapes could lead to the spherical or semi-spherical shapes of submicron particles during detachment from bulk material. Fig. 5 shows an example of particles from cast iron brake block and railway wheel contact where the flash temperature is considerably high. The authors also demonstrated that particle size distribution is time dependent and that, for various braking materials, the dominant peak can change with time.
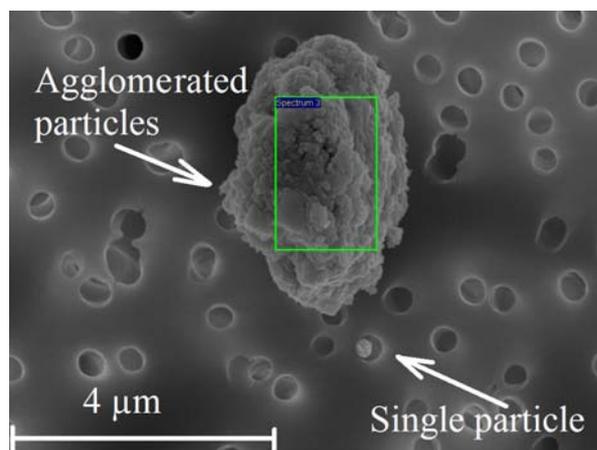
Fig. 5. An example of particle morphology from cast iron brake block and railway wheel (Abbasi *et al*, 2012b)

Another test investigated the effects of different lubricant and friction modifiers on airborne wear particles (Abbasi *et al*., 2013). The set-up, test conditions, and particle measurement instrumentation were similar to those used by Sundh *et al*. (2009). According to this work, the use of any friction modifiers reduces the generation rate of coarse particles. This effect was considerably stronger for biodegradable rail grease. However, the generation rate of ultrafine particle increased significantly when a water-based friction modifier was used.

3.2.3. Test rig studies

3.2.3.1. Road dust test rig

VTI simulated the operational contact conditions between tire and road in a test rig (Fig. 6) (Sjödin *et al*, 2011, Gustafsson *et al*. 2011). The set-up consists of four wheels running on a 5.3-m-diameter circular track. A DC motor drives each wheel at speeds of up to 70 km h^{-1}. This test rig can be used for any type of pavement and tire.

Fig. 6. A road simulator; image courtesy of VTI.

In one of their recent studies, Gustafsson *et al.* (2011) and Sjödin *et al.* (2011) tested summer tires, unstudded winter tires, and studded winter tires against eight different road pavement compositions (stone mastic asphalt). Three pavements with largest stone sizes of 8, 11, and 16 mm of porphyry and quartzite, and two pavements with largest stone sizes of 8 and 11 mm of mylonite were included in the test. In these test series, the tire inflation pressure was 2.5 bar, the normal weight was 450 kg, and the test cycle was based on running at 30, 50, and 70 km h^{-1} for 1.5, 1.5, and 2 h, respectively.

The main objective of these studies was to study the effects of rock material properties and stone size on PNC, PND, PMC and particle composition. A model 1400 TEOM (Thermo Scientific, Waltham, MA, USA) and a DustTrak 8520 laser photometer were used to measure PMC. An APS and an SMPS were used to measure PND. The APS, Model 3321 (TSI, Shoreview, MN, USA), was used to measure the PND of particles 0.5–20 μm in diameter every 20 s. The SMPS combined a model 3071 DMA and a model 3010 CPC. The detection range of SMPS was 7–297 nm. The particles were collected in a Nuclepore polycarbonate filter. A TEOM, equipped with a PM$_{10}$ inlet, works based on gravimetry using a microbalance and weighs the mass concentration every 5 min. An IVL invented sampler (IVL, Stockholm, Sweden) and an SDI cascade impactor (Dekati) were used to collect particles. The IVL sampler was used to collect particles in the PM$_1$, PM$_{2.5}$, and PM$_{10}$ fractions. The 47 mm diameter Zefluor filters, pore size 2 μm and 25 mm, and TF-1000 filter, pore size 1 μm were used to collect particles in the PM$_{10}$ and both PM$_{2.5}$ and PM$_1$ fractions. Two DustTrak 8520 equipped with omni-directional inlets were used to measure particles in the PM$_{10}$ and PM$_{2.5}$ fractions. The SDI was capable of collecting particles in the 0.045–8.39-μm range in 12 size intervals. The SFU was used to collect fine and coarse particles.

Two 47 mm diameter Nuclepore polycarbonate filters with pore sizes of 8 and 0.4 μm were used to collect the coarse and fine fractions, respectively. The PIXE method was used to investigate the element composition of the particles collected on the filters.

According to these tests, PM_{10} emissions in the road simulator are roughly 100 times higher for studded winter tires than for summer tires. Ultrafine particles were recorded only when studded tires were used. An increase in speed will increase the PM_{10} emissions, which decrease with increasing tire temperature and specific humidity for winter studded tires and unstudded tires, but increase with temperature for summer tires. The coarser fraction of PM_{10} emitted when using winter tires is dominated by mineral particles from the pavement, mainly comprising Si, but also Ca, K, and Fe. For summer tires, the relative contributions of Fe and Zn are equally important. S, which might originate from the tires and/or the pavement binder, usually forms a significant percentage of particles < 1 μm, while Zn, traceable to tire rubber, forms a significant percentage of particles > 1 μm. The element W also appears, originating from the studded tires. The results indicated that larger stones in the pavement, generally gives lower particulate emissions than smaller stones.

3.2.3.2. Brake test rig

Wahlström *et al*. (2009) used a test rig to simulate the dragging behavior of a car brake system (Fig. 7). Some brake systems are equipped with a drag system that make frequent low-pressure contact between brake pad and disc to ensure removal of dirt or rust layer.
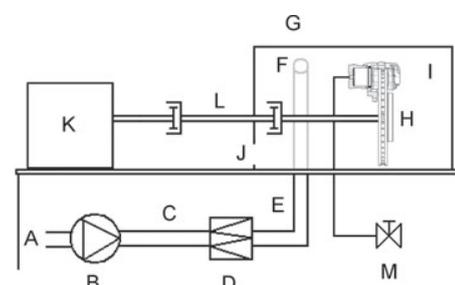
Fig. 7. A schematic view of the test system. The test rig is in a chamber; clean air is pumped into it after passing through a filter (Wahlström *et al*. 2009).

In this test, the LM and NAO brake pads were run against cast iron brake disc material, naturally coated with a rust layer. The rust layer was deliberately used to simulate the conditions of a car parked overnight in a wet environment. A Grimm 1.109 aerosol spectrometer, a P-Trak 8525 ultrafine particle counter, and a DustTrak 8520 laser photometer were used in the test. The rotational speed was 600 rpm and the pressure in the brake cylinder was 1.2, 1.7, and 2.2 bar.

According to this test, the PNC and PND were time dependent for both the NAO and LM samples. However, the dominant peaks, reported as 270 nm, 350 nm, 650 nm, and 3 μm, did not change with time.

4. Discussion and conclusion

Field testing produces the most realistic results, although the results may be quite complex requiring quite an extensive analysis effort. Furthermore, instrumenting a car or train is extremely costly, and due to safety concerns, it takes a long time to obtain permission to run a specially configured car or train. Most results from laboratory tests presented in the reviewed papers were in line with published results from field tests. However, the methods and results in all the papers had intrinsic limitations.

Using *dynamometers* to study the generation of wear particles is an interesting method. However, dynamometers can be used only at limited speeds. Besides, the effects of modern sliding-control systems, such as anti-slide/skid systems in trains or ABS and ASR systems in cars, which are

functionally dependent on track or road conditions and influence vehicle deceleration and consequently the airflow, can hardly be simulated by conventional dynamometers. Furthermore, the wide range of wheel housing shapes makes it a significant challenge to simulate the effect from real airflow in dynamometer tests.

Using a *pin-on-disc machine* in a sealed chamber is the most economical and flexible way to investigate wear-based airborne particles. In addition to the basic limitations of conventional pin-on-disc testing, such as limited speed and constant pressure, pin-on-disc studies are not capable of dealing with rolling contact and its effects. A pin-on-disc machine based studies have also limited capabilities to represent thermal fatigue. Furthermore, the thermal effects on the pins of a brake pad or brake block can be significantly greater than in the real situations, as the pin is smaller than real brake pads or brake blocks by an order of magnitude. Another limitation is that the thermo-mechanical effects of brake pads on discs and the airflow dynamics cannot easily be simulated in a pin-on-disc machine. The vertical orientation of brake discs in all ground vehicles could affect the formation of the tribochemical film, which can itself influence the characteristics of airborne particles (Abbasi, 2011).

To address these concerns, we suggest using a computer controlled pin-on-disc machine in a sealed chamber with a vertical rotating disc in particles from braking materials. The main advantage of a programming feature is to enable fully variable load and speed based on an approved protocol. In order to be able to record nominal contact temperatures, we also propose that an infra-red camera with emissivity correction according to Kasem's approach (Kasem *et al.*, 2010) should be mounted in the machine.

Constant speed, tight turns, dry conditions, limited speeds, and lack of the wheel sliding behaviour in ABS and ASR systems are also limitations of road test rigs. Furthermore, the real dynamic behaviour of the air in real road traffic cannot be reproduced by the *road dust test rig*.

It must be noted that omitting the true dynamic behaviour of the surrounding air can lead to quite misleading results. For example, Mosleh *et al*. (2004) reported that only 10% of brake-origin particles became airborne. They did, however, not consider external airflow in their testing. The results presented in (Augsburg *et al*., 2011) also confirms that the fluid dynamic behaviour of the air has a crucial influence on the characteristic properties of the generated airborne particles. The shift from a dominant particle size peak at 350 nm to one at 280 nm when braking at 80 km h^{-1} and at 180 km h^{-1} can also be discussed in terms of fluid dynamics, although this was not explicitly done by Abbasi et al. (2012c).

Another factor to consider in future studies is the transformation process of the emitted particles. According to results in (Wahlström *et al*., 2009, 2010b, Sjödin *et al*, 2011, Gustafsson *et al*. 2011, Abbasi *et al*. 2012b,c), PND and PVD are both time and temperature dependent, so measuring these characteristics requires particle measurement instruments with a high time resolution. In addition, new techniques are needed to sample airborne wear particles in real time for morphology and element composition studies. All recent studies have examined particles as collected on filters, studying them all together at the same time, neglecting *when* each particle was collected. There is also a lack of computerized imaging methods and tools for recording and classifying the morphology of the majority of particles based on shape factor parameters (Stachowiak, Stachowiak, & Podsiadlo, 2008). At the present time, SEM or FESEM can be used

to create sharp images of a limited number of particles. It can be misleading to take these images as representative of all particles, as the wear mechanism is neither constant over time nor the same for all wear particles.

Uncertainty is another important issue that was ignored in nearly all reviewed papers on wear particles. Bounanno et al. (2009) estimated the uncertainty of the PMC and PNC of particles in the 0.014–20-µm size range in field tests based on ISO/IEC Guide no. 98-3:2008. According to this work, the uncertainty of PMC and PNC measurements can reach 35% and 5%, respectively. These estimates were based on the assumption of spherically shaped particles and a predetermined average density for various sized particles. Obviously, wear particles are not exactly spherical and their densities can differ between size intervals. Consequently, the maximum uncertainty of the PMC and PNC of wear particles could well be higher than estimated. Yenisoy-Karakaş (2009) discussed the uncertainty of the element analysis of aerosols as determined using ICP-MS. They reported that the uncertainty for mass of the detected elements is 5–18% depending on sample size and element type.

In rail transport, wear particles are main source of PM in enclosed areas (Abbasi et al. 2012b, Abbasi, 2011). In contrast, exhaust particles from road transport, which are mainly carbon based, account for a greater proportion of the PM than do wear particles. However, wear particles can cause more adverse health effects than exhaust particles. Karlsson et al. (2005) reported that particles in subway systems (mainly wear-based) were eight times more genotoxic than road particles (mainly exhaust based).

Current exhaust emission directives such as Euro V and Euro VI and Tiers 2 and 4 impose emission limits that are progressively tightening over the years, gradually reducing total PM emitted by engines. Consequently, the relative contribution of wear particles to the PM levels is increasing gradually. There is also a general trend towards higher ground transportation speeds, which most likely cause higher wear and consequently more emitted wear particles. In view of this, there is a great need to improve the described laboratory testing techniques by defining flexible and controlled testing set-ups that enable more complex and real situations to be tested.

5. Acknowledgments

References

Abbasi, S. 2011, Characterization of airborne particles from rail traffic, Licenciate thesis, TRITA-MMK 2011:11, 2011, Sweden.

Abbasi, S., Wahlström, J., Olander, L., Larsson, C., Olofsson, U., & Sellgren, U. 2011. A study of airborne wear particles generated from organic railway brake pads and brake discs. *Wear, 273*(1), 93-99.

Abbasi, S., Jansson, A., Olofsson, U., and Sellgren, U. 2012a. Particle emissions from rail traffic: A literature review, *Critical Reviews in Environmental Science and Technology*, In press. Online version: http://dx.doi.org/10.1080/10643389.2012.685348

Abbasi, S., Jansson, A., Olander, L., Olofsson, U., & Sellgren, U. 2012b. A pin-on-disc study of the rate of airborne wear particle emissions from railway braking materials. *Wear, 284-285*, 18-29.

Abbasi, S., Olander, L., Larsson, C., Olofsson, U., Jansson, A., & Sellgren, U. 2012c. A field test study of airborne wear particles from a running regional train. *Proceedings of the Institution of Mechanical Engineers, Part F: Journal of Rail and Rapid Transit, 226*(1), 95-109.

Abbasi, S., Olofsson, U. and Sellgren, U. 2013. Pin-on-disc study of the effects of railway friction modifiers on airborne wear particles from wheel–rail contact, *Tribology International*, 60, 136-139.

Augsburg, K., Gramstat, S., Horn, R. and Sachse. H., 2011. Measures Development for Brake Dust Emissions with Computational Fluid Dynamics and Particle Imaging Velocimetry. SAE International.

Buonanno, G., M. Dell'Isola, L. Stabile, and A. Viola. 2009. Uncertainty budget of the SMPS-APS system in the measurement of PM 1, PM 2.5, and PM 10. *Aerosol Science and Technology* 43:1130-1141.

EPA NAAQS, 2012. National Ambient Air Quality Standards . Available at http://www.epa.gov/pm/2012/decfsoverview.pdf (accessed 15 December 2012).

EU Directive 2008/50/EC, 2008. On ambient air quality and cleaner air for Europe. Available at http://eur-lex.europa.eu/LexUriServ/LexUriServ.do?uri=OJ:L:2008:152:0001:0044:EN:PDF (accessed 21 February 2012).

Garg, B. D., S. H. Cadle, P. A. Mulawa, P. J. Groblicki, C. Laroo, and G. A. Parr. 2000. Brake wear particulate matter emissions. *Environmental Science and Technology* 34:4463-4469.

Gustafsson, M.; Blomqvist, G., Gudmundsson, A., Jonsson, P., Swietlicki, E. (2011), Vägbeläggningars damningsbenägenhet, VTI Rapport 711, Sweden (http://www.vti.se/sv/publikationer/vagbelaggningars-damningsbenagenhet/)

Hopke, P. K. 2009. Contemporary threats and air pollution. *Atmospheric Environment* 43:87-93.

Karlsson, H. L., L. Nilsson, and L. Möller. 2005. Subway particles are more genotoxic than street particles and induce oxidative stress in cultured human lung cells. *Chemical Research in Toxicology* 18:19-23.

Kasem, H., Thevenet, J., Boidin, X., Siroux, M., Dufrenoy, P., Desmet, B., & Desplanques, Y. 2010. An emissivity-corrected method for the accurate radiometric measurement of transient surface temperatures during braking. *Tribology International, 43*(10), 1823-1830.

Mosleh, M., P. J. Blau, and D. Dumitrescu. 2004. Characteristics and morphology of wear particles from laboratory testing of disk brake materials. *Wear* 256:1128-1134.

Olofsson, U., Olander, L. and Jansson, A., 2009. A study of airborne wear particles generated from a sliding contact. *Journal of Tribology*, 131(4):1-4.

Olofsson, U. 2011. A study of airborne wear particles generated from the train traffic-Block braking simulation in a pin-on-disc machine. *Wear* 271:86-91.

Sjödin, Å., Ferm, M., Björk, A., Rahmberg, M., Gudmundsson, A., Swietlicki, E., Johansson, C., Gustafsson, M., Blomqvist, G., (2011), Wear particles from road traffic: a field, laboratory and

modelling study, Report B1830, IVL, Swden (http://www.ivl.se/webdav/files/B-rapporter/B1830.pdf).

Stachowiak, G. P., Stachowiak, G. W., & Podsiadlo, P. (2008). Automated classification of wear particles based on their surface texture and shape features. *Tribology International*, *41*(1):34-43.

Sundh, J., U. Olofsson, L. Olander, and A. Jansson. 2009. Wear rate testing in relation to airborne particles generated in a wheel-rail contact. *Lubrication Science* 21:135-150.

Thorpe, A. and R. M. Harrison. 2008. Sources and properties of non-exhaust particulate matter from road traffic: A review. *Science of the Total Environment* 400:270-282.

Wahlström, J., A. Söderberg, L. Olander, A. Jansson, and U. Olofsson. 2010a. A pin-on-disc simulation of airborne wear particles from disc brakes. *Wear* 268:763-769.

Wahlström, J., A. Söderberg, L. Olander, and U. Olofsson. 2009. A disc brake test stand for measurement of airborne wear particles. *Lubrication Science* 21:241-252.

Wahlström, J., A. Söderberg, L. Olander, U. Olofsson, and A. Jansson. 2010b. Airborne wear particles from passenger car disc brakes: A comparison of measurements from field tests, a disc brake assembly test stand, and a pin-on-disc machine. *Proceedings of the Institution of Mechanical Engineers, Part J: Journal of Engineering Tribology* 224:179-188.

Yenisoy-Karakaş, S., E. O. Gaga, O. Cankur, and D. Karakaş. 2009. Uncertainty of high resolution inductively coupled plasma mass spectrometry based aerosol measurements. *Talanta* 79:1298-1305.